Carbohydrate Polymers 96 (2013) 593–601

Contents lists available at SciVerse ScienceDirect

Carbohydrate Polymers

journal homepage: www.elsevier.com/locate/carbpol

Characterization of starch films containing starch nanoparticles Part 1: Physical and mechanical properties

Ai-min Shi [a,1], Li-jun Wang [b,1], Dong Li [a,*], Benu Adhikari [c]

[a] College of Engineering, China Agricultural University, P. O. Box 50, 17 Qinghua Donglu, Beijing 100083, China
[b] College of Food Science and Nutritional Engineering, China Agricultural University, Beijing, China
[c] School of Health Sciences, University of Ballarat, VIC 3353, Australia

ARTICLE INFO

Article history:
Received 26 August 2012
Received in revised form 8 December 2012
Accepted 11 December 2012
Available online 27 December 2012

Keywords:
Corn starch film
Starch nanoparticles
Physical properties
Mechanical properties

ABSTRACT

We report, for the first time, the preparation method and characteristics of starch films incorporating spray dried and vacuum freeze dried starch nanoparticles. Physical properties of these films such as morphology, crystallinity, water vapor permeability (WVP), opacity, and glass transition temperature (T_g) and mechanical properties (strain *versus* temperature, strain *versus* stress, Young's modulus and toughness) were measured. Addition of both starch nanoparticles in starch films increased roughness of surface, lowered degree of crystallinity by 23.5%, WVP by 44% and T_g by 4.3 °C, respectively compared to those of starch-only films. Drying method used in preparation of starch nanoparticles only affected opacity of films. The incorporation of nanoparticles in starch films resulted into denser films due to which the extent of variation of strain with temperature was much lower. The toughness and Young's modulus of films containing both types of starch nanoparticles were lower than those of control films especially at <100 °C.

1. Introduction

Starch-based films have drawn considerable attention due to their potential application in producing agricultural foils, garbage or composting bags, food packaging and edible films (Yun & Yoon, 2010). Starch-based films can be produced by adding judicious amount of plasticizers and using either hot melt processing or solution casting (Bengtsson, Koch, & Gatenholm, 2003; Kampeerapappun, Aht-ong, Pentrakoon, & Srikulkit, 2007; Wilhelm, Sierakowski, Souza, & Wypych, 2003). The addition of plasticizers such as formamide (Dai, Chang, Geng, Yu, & Ma, 2010), sorbitol (Galdeano, Mali, Grossmann, Yamashita, & García, 2009), xylitol (Vieira, da Silva, dos Santos, & Beppu, 2011), glycerol (Kampeerapappun et al., 2007), and glycerol and xylitol in combination (Muscat, Adhikari, Adhikari, & Chaudhary, 2012) considerably improves mechanical properties such as tensile strength, strain at break, flexibility and modulus of elasticity. Even though the presence of plasticizers improves these mechanical properties of starch films, due to hydrophilic nature of starch and its sensitivity to moisture and heat, further modification is usually necessary.

There are many methods that can be used to modify the structure and function of starch-based films. Among these methods, blending with other compounds in the film forming solution is a useful way to modify the structure and properties of starch-based films (Briassoulis, 2004). Many materials such as chitosan (Bourtoom & Chinnan, 2008; Zhai, Zhao, Yoshii, & Kume, 2004), protein (Jagannath, Nanjappa, Das Gupta, & Bawa, 2003; Ryu, Rhim, Roh, & Kim, 2002), polyvinyl alcohol (PVA) (Follain, Joly, Dole, & Bliard, 2005; Jayasekara, Harding, Bowater, Christie, & Lonergan, 2004), and poly-3-hydroxybutyrate (PHB) (Godbole, Gote, Latkar, & Chakrabarti, 2003) have been successfully used to produce starch-based films having some tailored properties.

In addition, a plethora of micro- or nano-particles can be used to blend with the starch suspension to produce starch-based films. Wittaya (2009) reported the preparation method and characteristics of rice starch films reinforced with microcrystalline cellulose from palm pressed fiber. Xiong, Tang, Tang, and Zou (2008) added nano-SiO_2 in starch-based biodegradable film and reported that the tensile strength, elongation at break, and transmittance increased by 79.4%, 18%, and 15%, respectively. Interestingly, the water absorption was found to decrease by 70% due to the addition of nano-SiO_2. Byun, Park, Lim, and Yoon (2011) studied the effect of the presence of nano-sized poly(acrylamide-co-methyl methacrylate) (PAAm-co-MMA) and nano-sized TiO_2 (P-25)/PAAm-co-MMA composite in starch-based films. These authors studied the morphology, crystallinity, physical and mechanical properties, and photocatalytic degradability of the above mentioned films and reported that the presence of micro- and nano-particles significantly affects the physical and mechanical properties.

* Corresponding author. Tel.: +86 10 62737351; fax: +86 10 62737351.
E-mail address: dongli@cau.edu.cn (D. Li).
[1] These authors contributed equally to this work.

0144-8617/$ – see front matter © 2012 Elsevier Ltd. All rights reserved.
http://dx.doi.org/10.1016/j.carbpol.2012.12.042

However, the formation and characteristics of starch-based films containing starch nanoparticles, to our knowledge, are not reported so far. Starch nanoparticles (StNPs) or nanospheres are nano-sized (1–1000 nm) particulates of starch prepared by chemically cross-linking starch molecules with appropriate cross-linkers (Le Corre, Bras, & Dufresne, 2010). We previously reported that the starch nanoparticles can be successfully produced using the water-in-oil (w/o) mini-emulsion cross-linking technique using a high pressure homogenizer (Shi, Li, Wang, Li, & Adhikari, 2011). Because starch is the major component in both the starch nanoparticle and starch-based films, it is expected that the blending or mixing of starch nanoparticles in starch-based films would be easier than other compounds having dissimilar molecules. Hence, it is expected that the production of starch-based films containing starch nanoparticles would be practicable.

In this first part, we attempted to produce starch films with and without starch nanoparticles and investigate their physical properties such as morphology, amorphous/crystalline nature, WVP, opacity, and glass transition temperature and mechanical properties (strain as a function of stress, Young's modulus, toughness and strain as a function of temperature). Spray dried and vacuum freeze dried starch nanoparticles were incorporated in the starch films to understand the impact of drying methods used to prepare the nanoparticles.

2. Materials and methods

2.1. Materials

Corn starch was obtained from Hebei Zhangjiakou Yujing Food Co. Ltd. (Hebei, China). Glycerol (analytical grade) was purchased from Beijing Chemical Reagent Ltd. (Beijing, China). Xylitol (food grade) was purchased from Tianjin Jinguigu Science & Technology Development Co. Ltd. All these materials were used as received.

2.2. Preparation of starch nanoparticles

Starch nanoparticles were produced following the emulsion cross-linking method using a high pressure homogenizer (Shi et al., 2011). Spray drying and vacuum freeze drying techniques were used to prepare starch nanoparticles (Shi, Li, Wang, Zhou, & Adhikari, 2012; Shi, Wang, Li, & Adhikari, 2012).

2.2.1. Spray drying

A bench-top spray dryer (GPW120-II, Shandong Tianli Drying Equipment Co., Ltd., Shandong, China) with 500 mL/h evaporation capacity was used throughout the spray drying trials. The atomization of the droplet was accomplished using a 0.7 mm two-fluid nozzle and compressed air was used as atomizing medium. The flow rate of the compressed air was 10 L/min and its pressure was maintained at 608 kPa. The feed flow rate and inlet temperature were set at 5.4 mL/min and 100 °C, respectively. The powders were collected at the cyclone and finally transferred to resealable snap lock bags. These spray dried starch nanoparticles were stored in a desiccator containing dried allochroic silica gel at 25 °C.

2.2.2. Vacuum freeze drying

A laboratory-scale vacuum freeze dryer (LGJ-18, Sihuan, China) was used to dry the starch nanoparticles. The sample dishes ($0.1\,m^2 \times 3\,cm$) containing the suspension ($0.1\,m^2 \times 1\,cm$) were placed in the cold trap of the vacuum freeze dryer (−60 °C) for 5 h to ensure complete freezing of the sample. Subsequently, the frozen samples were placed in drying chamber and then the chamber was evacuated (<100 Pa). The temperature of frozen samples was varied from −30 °C to 45 °C step by step in the 28 h-long drying period (1 h each at −30 °C, −25 °C, −20 °C, −15 °C, −10 °C, −5 °C; 2 h each at 0 °C, 5 °C, 10 °C, 15 °C, 20 °C, 25 °C, 30 °C, 35 °C, 40 °C and finally 4 h each at 45 °C). The vacuum freeze dried starch nanoparticles were stored in the same desiccator in which spray dried samples were stored.

2.3. Film preparation

7.0 g of previously dried (40 °C for 6 h) cornstarch and 3.0 g of plasticizers (glycerol and xylitol, 1:1) was added into 200 ml deionized water to form starch-plasticizer dispersions with 5.0 wt.% (w/v) solid concentration. The dispersion batches were thoroughly stirred at 300 rpm (in beakers) for 1 h using a thermostated water bath in boiling condition. Evaporation was minimized by covering the beakers with six layers of water resistant films. After gelatinizing the starch at 100 °C for 1 h and cooling to 70 °C, 0.5 wt.% (w/v) starch nanoparticles was added into the dispersions (Fu, Wang, Li, Wei, & Adhikari, 2011). These dispersions, after introducing the starch nanoparticles, were further stirred for 30 min at 300 rpm. The dispersions having no starch nanoparticles in them severed as the control sample.

Films were cast by syringing 8 mL of the above mentioned dispersions into 9 cm diameter polycarbonate petri dishes. Films were dried for over 8 h at 45 °C. All the dried starch film were preserved in a humidity chambers (25 °C, RH = 53%) for further testing. The nomenclature of these films is presented in Table 1.

2.4. Physicochemical properties

2.4.1. Morphology

Film surface morphology was examined using a scanning electron microscope (S-3400N, Hitachi Instruments Ltd., Japan). Films were firstly dried at 100 °C for 12 h. Then these dried film samples were mounted on stub with double-sided adhesive tape and coated with a thin layer of gold. The surface characteristics of the samples was observed and recorded under S-3400N using an accelerating voltage of 15 kV and a 5000× magnification.

2.4.2. X-ray diffraction (XRD)

The amorphous/crystalline structure of the sample was examined using an X-ray diffractometer (XD-2, Beijing Purkinje General Instrument Co., Ltd., China). It used nickel filtered Cu Kα radiation ($\lambda = 0.15406$ nm) and worked at a voltage of 36 kV and current of 20 mA. The slit width of 1° and the 2θ range from 5° to 45° in steps of 0.02°/s were used. The starch film samples were cut into pieces and pulverized using a laboratory grinder. The pulverized sample was further dried in a laboratory oven (105 °C) for 6 h to remove the moisture. The dried powder sample was compacted to form an even surface before loading to the XRD instrument. The temperature and relative humidity (RH %) for tests were 25 °C and 20%, respectively.

2.4.3. Water vapor permeability (WVP)

The ASTM method E96-80 with some modifications (ASTM, 1987) was used to measure WVP of the films. Each film sample was sealed over a circular opening (area = 0.000632 m^2) in a permeation cell that was conditioned at 25 °C in a desiccator. As outlined in the standard method, anhydrous calcium chloride (0% RH) was placed inside the cell while a saturated sodium chloride solution (75% RH) was placed in the desiccator. Due to the vapor pressure gradient across the film, the water vapor continuously diffuses through the film and the water vapor transmission rate can be determined from the weight gained by the permeation cell. The change in the weight of the cell was measured every 24 h over a week.

The change in the weight of the cell was plotted as a function of time and the slope of each line was calculated by linear regression. The water vapor transmission rate (WVTR) was calculated from

Table 1
The WVP, opacity and T_g of starch films containing spray and vacuum freeze dried starch nanoparticles (RH = 51%).[+]

Film type	Composition (except starch)	WVP[*] (10^{-7} g Pa^{-1} h^{-1} m^{-1})	Opacity[*] (AU nm)	T_g[*] (°C)
B Film	Control	2.595 ± 0.054[a]	24.452 ± 0.754[a]	43.0 ± 1.6[a]
S Film	Spray dried starch nanoparticles	1.491 ± 0.193[b]	23.965 ± 0.146[a]	39. 1 ± 0.7[b]
F Film	Vacuum freeze dried starch nanoparticles	1.454 ± 0.138[b]	30.499 ± 0.037[b]	38.7 ± 0.9[b]

[+] Values represent the mean ± standard deviation of triplicate tests. Values in a column with different superscripts were significantly different ($P < 0.05$).
[*] WVP represents the water vapor permeability; *Opacity* represents the light with wavelength ranged from 400 nm to 800 nm); T_g represents the glass transition temperature.

the slope (g/s) and the cell area (m^2). After these permeation tests, film thickness was measured and the WVP (g Pa^{-1} h^{-1} m^{-1}) was calculated. WVTR and WVP are determined using Eqs. (1) and (2) (Hu, Topolkaraev, Hiltner, & Baer, 2001; Muscat et al., 2012).

$$\mathrm{WVTR} = \frac{1}{A}\left(\frac{\Delta W}{t}\right) \quad (1)$$

$$\mathrm{WVP} = \frac{\mathrm{WVTR} \times x}{P \times (R_1 - R_1)} \quad (2)$$

Here, ΔW is the weight change of the cell (g); t is the time (h); A is the test area (m^2); P is the saturation vapor pressure of water (3.169×10^3 Pa at 25 °C); R_1 and R_2 are the relative humidity (RH) values in the desiccators and the permeation cell (expressed in fraction), respectively. Similarly, x is the film thickness (m). All of these tests were carried out in triplicate.

2.4.4. The film opacity

The opacity of the films was determined using a modified BSI standard procedure (1968) (Mali, Grossmann, García, Martino, & Zaritzky, 2004) using an UV–vis spectrophotometer (TU-1810, Beijing Purkinje General Instrument Co., Ltd., Beijing, China). Film samples [40 mm (length) × 10 mm (width) × 0.1–0.5 mm (thickness)] were placed in the inner side of the spectrophotometer cell to record the absorbance spectrum between 400 and 800 nm. Opacity of the films was defined as the area under the curve and expressed as absorbance unit × nanometers (AU nm). All the tests were conducted in quadruplicate ($n = 4$).

2.4.5. Measurement of glass transition temperature (T_g)

The T_g of each film sample was measured using a differential scanning calorimeter (DSC) (Q10, TA Instruments Ltd., New Castle, DE). Film sample was crushed and 4–6 mg of film mass was weighed in aluminum pans and sealed using aluminum caps. The thermal analyses were performed in two-cycle mode, covering a temperature range of −25 °C to 100 °C (Shi, Li, et al., 2012; Shi, Wang, et al., 2012). A heating rate of 10 °C/min was used throughout. Nitrogen was used as flushing gas. The first heating cycle was used to remove the thermal history of the samples. The thermograms obtained from second heating cycle were used to determine the T_g using Universal Analysis 2000 data analysis software (TA Instruments Ltd., New Castle, DE).

2.5. The mechanical tests

2.5.1. Temperature sweep tests

The temperature sweep tests were conducted by using a dynamic mechanical analyzer (DMA, Q800, TA Instruments, New Castle, USA) in tension mode using film clamps. The film for DMA analysis was cut into 50 mm × 10 mm strips (average thickness, 0.1–0.5 mm). The strip was placed in tension between a fixed and moveable clamp while a small static force (0.02 N) was applied in order to prevent buckling (Pandini et al., 2012). Subsequently, a fixed static force (0.1 N) was used to stretch the film and the variation of strain with increase in temperature was record. The strain *versus* temperature data were plotted using the Universal Analysis 2000 data analysis software (TA Instruments Ltd., New Castle, DE). The temperature was ramped up from 30 °C to 150 °C at a rate of 3 °C/min.

2.5.2. Stress sweep tests

Stress sweep tests were carried out in these films the dynamic mechanical analyzer (DMA, Q800, TA Instruments, New Castle, DE) using film tension clamps. The specification of the film samples in these tests was the same as was in temperature sweep tests. The film strip was then clamped into the DMA furnace at both ends and the actual gap between both ends was measured with a small preload force of 0.02 N. The uniaxial tensile tests were conducted using a loading stress rate of 5 MPa/s at a frequency of 1 Hz in five temperature settings (30 °C, 60 °C, 90 °C, 120 °C and 150 °C). Other test conditions such as static force (0.02 N) and force track (125%) were identical in all these tests. The tests were continued until the fracture occurred. Then the strain-stress curves were plotted using the Universal Analysis 2000 data analysis software as mentioned before. The relationship between the tensile stress and tensile strain (Hooke's Law) is given by Eq. (3), below.

$$\sigma_e = E\varepsilon_e \quad (3)$$

where σ_e represents the tensile stress (Pa), ε_e represents the tensile strain (dimensionless), E represents the Young's modulus or modulus of elasticity (Pa).

The Young's modulus (E) was calculated using Eq. (3) from the slope of initial linear portion of the stress–strain curve (Cheng, Catchmark, & Demirc, 2011; Roylance, 2001). Toughness (J) is defined as the amount of energy that a film absorbs before yielding. This is an important parameter which was obtained from the area under the stress–strain curve using the Origin 7.5 software (OriginLab Corporation, Northampton, MA) (Safranski, Crabtree, Huq, & Gall, 2011).

2.6. Statistical analysis

Duncan's multiple comparison method was used to determine the significant difference between mean values. A confidence level was set at $P < 0.05$ and the SAS software (SAS Institute Inc., Cary, NC, USA) was used in these statistical analyses.

3. Results and discussion

3.1. Physical properties

3.1.1. Film surface morphology

Fig. 1 presents the SEM morphology of the starch-only (control, Panel A), starch film incorporating starch nanoparticles (Panels B and C) and the morphology of spray dried (Panel D) and vacuum freeze dried (Panel E) starch nanoparticles. Fig. 1(A) shows that the surface of starch film in the absence of starch nanoparticle is smooth. This can be attributed to the presence of plasticizers during the formation of the dispersions and the films. However, Fig. 1(B) and (C) shows many protuberances or particles in the surface which make the surface uneven and rough. Compared with the size and

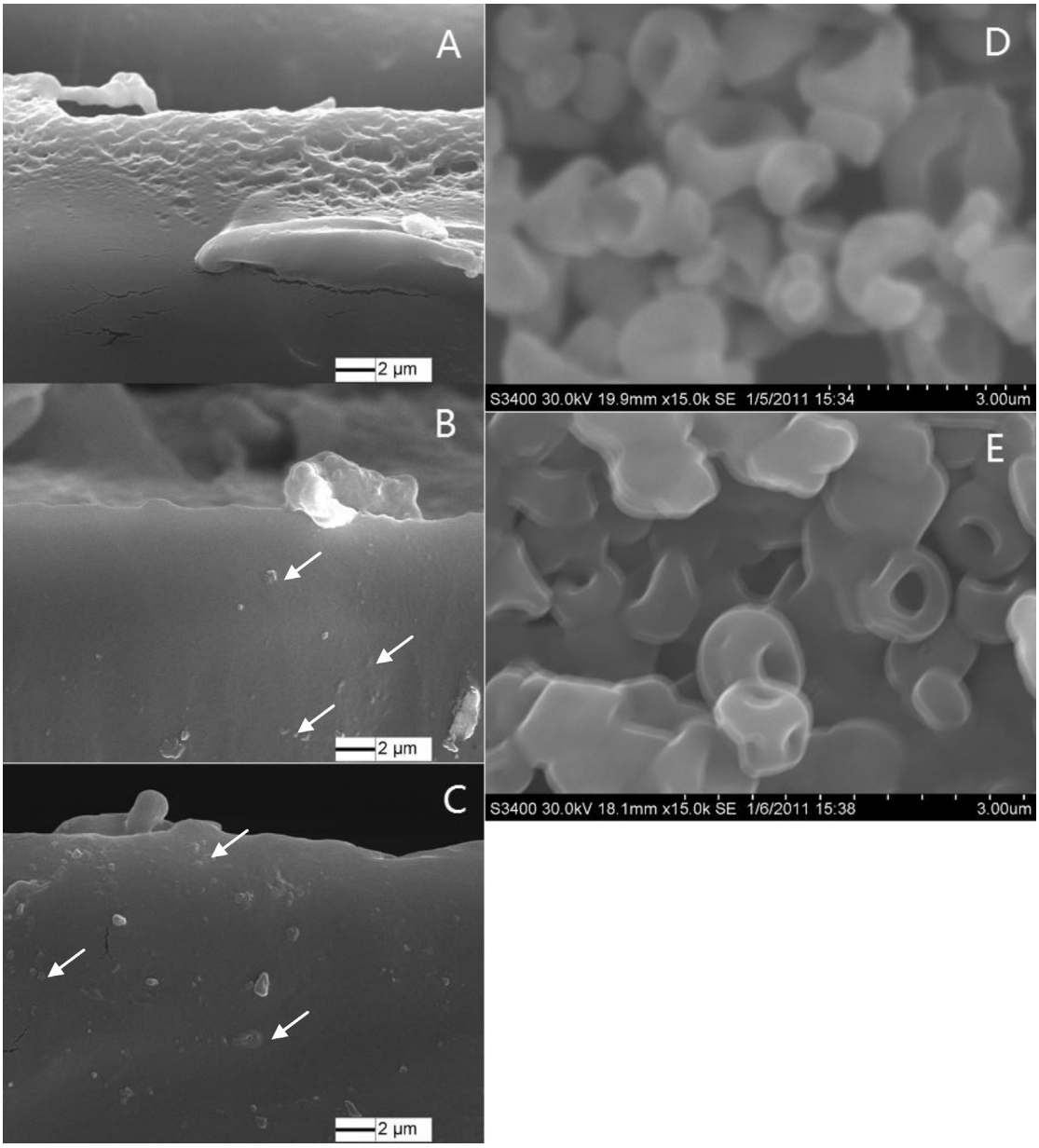

Fig. 1. SEM microphotographs of starch film and starch nanoparticles. (A) represents the microphotograph of the control film; (B) represents the film which incorporates spray dried starch nanoparticles; (C) represents the film which incorporates vacuum freeze dried starch nanoparticles; (D) and (E) represent the morphology of spray dried and vacuum freeze dried starch nanoparticles, respectively.

morphology of starch nanoparticles in Fig. 1(D) and (E), it can be suggested that these protuberances are resulted from the presence of starch nanoparticles. Furthermore, the presence of nanoparticles produced through the spray drying and freeze drying methods had identical effect on the surface morphology of the starch films.

3.1.2. Amorphous/crystalline nature

The wide angle X-ray diffraction patterns of starch films in the presence and absence of the nanoparticles and the diffraction patterns of starch nanoparticles in between 5° (2θ) and 45° (2θ) are shown in Fig. 2. As can be seen from Fig. 2(A), the X-ray diffraction pattern of the film B (control sample) shows the characteristic peaks at 16° (2θ), 20° (2θ) and 21° (2θ). This diffraction pattern is in accordance with the XRD pattern of corn starch the only difference being the fact that the peak at 25° (2θ) has disappeared (Lawal, Adebowale, Ogunsanwo, Barba, & Ilo, 2005). Interestingly, the characteristic diffraction peaks of the corn starch have almost disappeared in Fig. 2(B) and (C) due to the addition of starch nanoparticles. The diffractograms presented in Fig. 2(D) and (E) show that the starch nanoparticles produced through both the spray drying and vacuum freeze drying methods are amorphous in nature. In addition, the peak at 33° (2θ) in these two figures represents the existence of NaCl as explained in our previous research (Shi, Li, et al., 2012; Shi, Wang, et al., 2012). It appears that the presence of starch nanoparticles in film forming dispersion prevents the crystallization of starch or formation of crystalline regions in the starch films containing these nanoparticles. The mechanism with which these starch nanoparticles prevent the crystallization of starch is not yet understood. However, it is expected that there may be three way interactions among incorporated nanoparticles, plasticizer and starch (Saiah, Sreekumar, Leblanc, Castandet, & Saiter, 2007). It appears that the type of drying methods used to produce

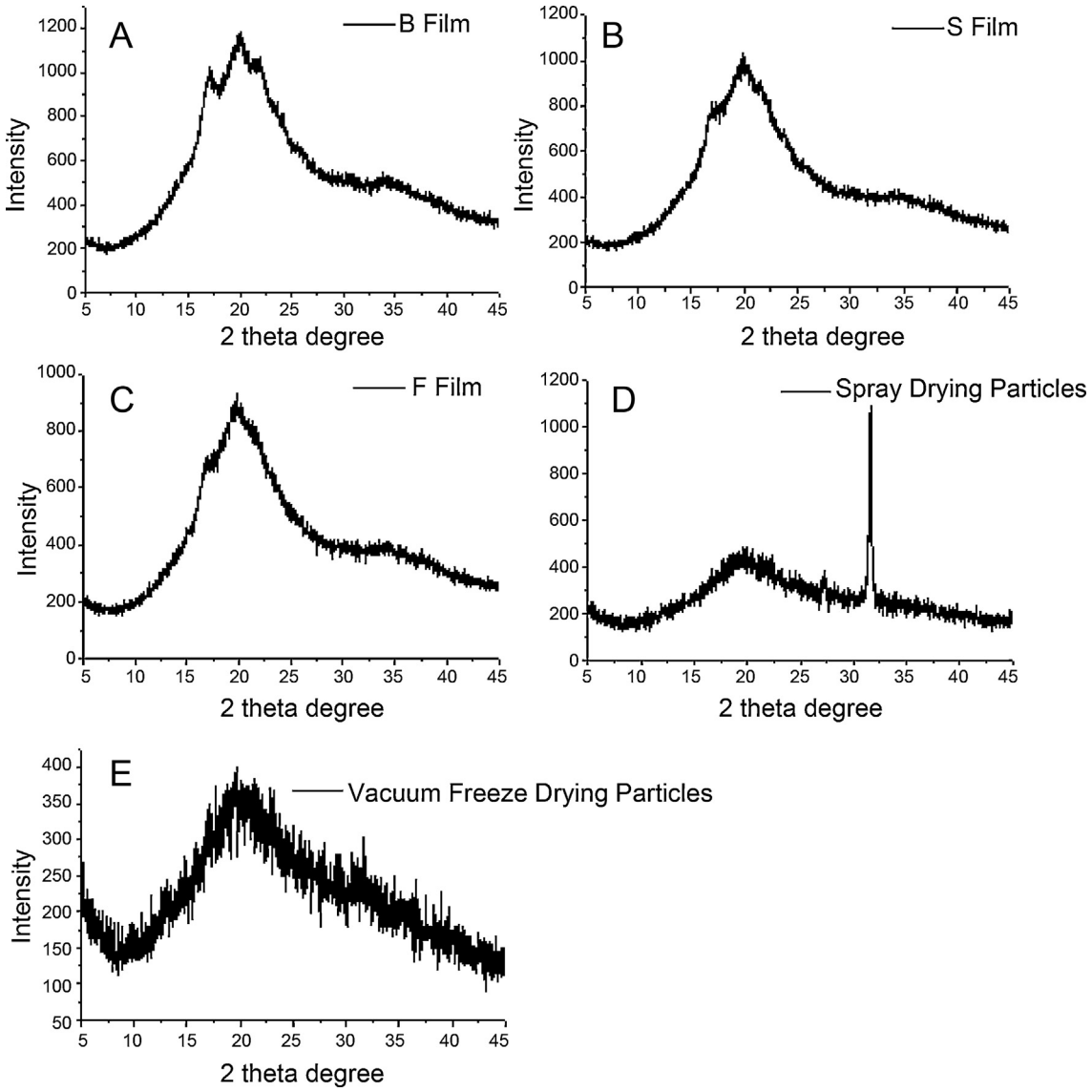

Fig. 2. X-ray diffraction patterns of starch film and starch nanoparticles. (A) starch-only control film; (B) film containing spray dried starch nanoparticles; (C) film containing freeze dried starch nanoparticles; (D) spray dried starch nanoparticles; (E) vacuum freeze dried starch nanoparticles.

the nanoparticles does not seem to make any perceived difference in formation of non-crystalline starch film containing these nanoparticles.

3.1.3. Water vapor permeability (WVP)

The WVP values of the films with and without the addition of starch nanoparticles are presented in Table 1. As can be seen from this table, the WVP of control film (with no incorporation of starch nanoparticles) is 2.595×10^{-7} g Pa^{-1} h^{-1} m^{-1} which is significantly ($P < 0.05$) higher than the WVP of starch films containing spray dried and vacuum freeze dried starch nanoparticles. The enhancement in water vapor resistance might have been resulted from the fact that the nanoparticles increase the compactness of the films owing to their very small size. It has been previously reported that the nanoparticles can prevent the formation of intermolecular hydrogen bonding amongst starch molecules which can reduce the water vapor diffusion through the film (Xiong et al., 2008). The WVP values of the films containing spray dried and spray freeze dried starch nanoparticles were very close to each other ($P > 0.05$) which further suggests that the drying methods involved in production of the starch nanoparticles do not have significant impact on the WVP of the starch films containing these starch nanoparticles films.

3.1.4. The opacity of the films

The opacity of starch films were quantified using spectral scanning with wavelength varying from 400 nm to 800 nm (Table 1). As can be seen from this table, the film containing vacuum freeze dried starch nanoparticles has the highest opacity (30.499 AU nm) ($P < 0.05$) while the films containing spray dried starch nanoparticles has the lowest opacity value (23.965 AU nm) ($P > 0.05$). These results indicate that these two drying methods do introduce some differences in the physical structure of the starch nanoparticles which ultimately affects the three-way interaction amongst starch, plasticizer and the starch nanoparticles during film formation. The possible reason for higher opacity value in films containing vacuum freeze dried starch nanoparticles is due to the fact that mean particle size of spray dried starch nanoparticles is much larger than the size of the interspace in starch film while the mean particle size of vacuum freeze dried starch nanoparticles is almost similar to the size of the interspaces in starch film. When the light passes through these films, much lower extent of light is transmitted through the

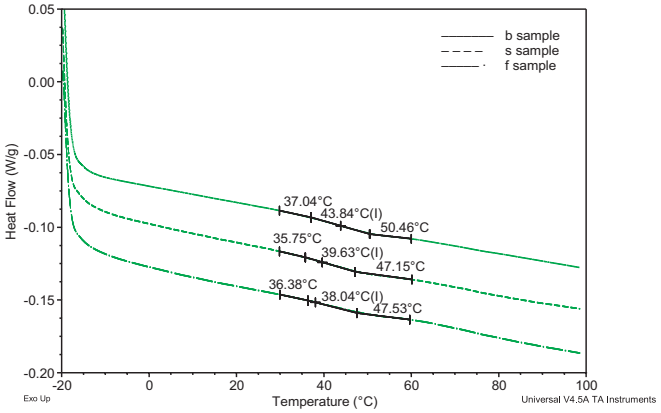

Fig. 3. Thermogram of starch film with and without starch nanoparticles.

film containing vacuum freeze drying starch nanoparticle which results into higher opacity value. The fact that the films containing spray dried starch nanoparticles had similar opacity value to that of starch-only film explains the fact that the interspace values in these two film samples are similar.

3.1.5. T_g of the films

The T_g values of starch film with and without starch nanoparticles are listed in Table 1. And the thermograms of starch films are displayed in Fig. 3. As can be seen from this table, the control film shows the highest T_g value (43.0 °C at RH = 51%). This value is higher than the T_g (35.0 °C) of corn starch-glycerol film (corn starch:glycerol = 83:17, w/w) at 10.9% (w/w) moisture content (Talja, 2007). This might have been resulted from the higher proportion of xylitol in our formulation as the xylitol has much higher T_g (−23.2 °C) than that of glycerol (−90 °C) (Muscat et al., 2012). The T_g values of the films containing spray dried and vacuum freeze dried starch particles are not significantly ($P > 0.05$) different. The T_g values of these films were slightly lower compared to that of the control film (B Film). It is now established that the increase in percentage of low molecular weight plasticizes in the blend lowers T_g of the starch films (Talja, 2007).

3.2. Mechanical properties

3.2.1. The strain of the films as a function of temperature

The evolution of the strain of starch film with and without starch nanoparticles with the ramping up of the temperature from 30 °C to 150 °C at a rate of 3 °C/min is shown in Fig. 4. In the case of control film (B Film), the strain increases immediately with the application of the static force (0.1 N) at 30 °C. After attaining the highest value (0.61%) at 37.5 °C, the strain of the control film decreases rapidly to the lowest value (−1.15%) at 120 °C. Then the strain starts to increase when the temperature increases from 120 °C to 150 °C. In the case of films containing spray dried and freeze dried starch nanoparticles the magnitude and trend in the variation of strain with temperature are quite similar while both are quite different compared to those of the control films. Specifically, their strains increase to the first high value very slowly when the temperature increased from 30 °C to 75 °C. Subsequently, when the temperature increased from 75 °C to 150 °C, the strains decreased first and then increased to the highest value. As can be seen from Fig. 4, the S Film had higher strain values than those of F Film over the entire temperature range studied (30–150 °C).

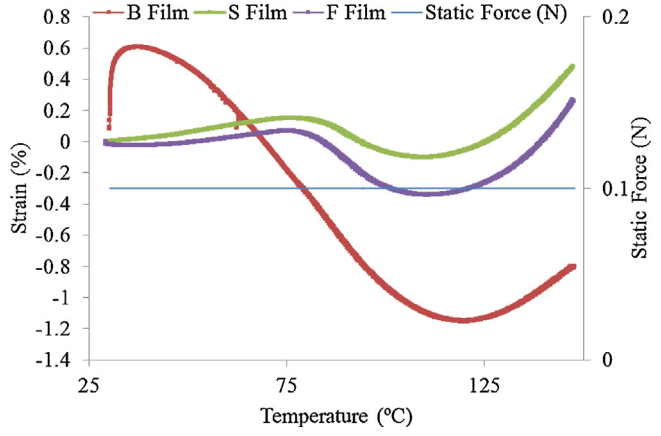

Fig. 4. The temperature sweep tests of starch films in the absence and presence of starch nanoparticles at a controlled force ($F = 0.1$ N).

As discussed in Section 3.1.2, the amorphous/crystalline nature of the films in the presence and absence of starch nanoparticles was quite different. As the starch nanoparticles act as the filler in these films, they can randomly occupy inter or intra molecular space which results into greater densification of the films. In other word, the presence of starch nanoparticles brings about densification in the film which ultimately results into lesser degree deformation (Xiong et al., 2008). This means that the variation of strain (in these nanoparticles containing films) with temperature will not be as sensitive as in the case of control film. This explains the fact that rapid increase of strain observed in the control (B Film) was not observed in S Film and F Film.

It has to be mentioned here that some degree of moisture evaporation takes place from these films during temperature sweep experiments. This leads to some degree of shrinkage in the film which is expected to affect the variation of strain with temperature due to the reduction in surface energy (Steward, Hearn, & Wilkinson, 2000). This is the reason why the strain decreases to such extent when the temperature increases from 35 °C to 100 °C. When the starch-only film (B Film) dries out due to continuous increase in the temperature these films shrinks to its limit after which the variation in the strain is very slow (Fig. 4). Above 120 °C, the starch molecules show stretching and increased mobility making the film much more ductile and flexible. This might explain why the strain of B Film increased further above 120 °C.

Furthermore, the higher compactness or densification in the films containing spray and freeze dried starch nanoparticles can also provide them with ability to resist or slow down the effect on strain when the temperature increases. After a slow increase of strain in films containing both the spray dried and vacuum freeze dried nanoparticles, these films are also seemingly affected by the loss of water. The densification in S Film and F Film is not adequate to prevent the temperature induced shrinkage of film when the temperature increases from 75 °C to 100 °C. The shrinking of the film causes the reduction of strain in both S Film and F Film. The lower values of strain in S Film and F Film might have also resulted from the loss of moisture in these films. And the higher densification of S Film and F Film could be the reason for the earlier appearance of the lowest strain. When the temperature of the films increases above 100 °C, it increases the mobility of starch molecules and the film matrix softens considerably. This softening of starch matrix enhances the flexibility of film which can be seen in substantial increase in the strain values (Chen, Liu, Chang, Anderson, & Huneault, 2008; Glenn, Imam, & Orts, 2011). This softening of the film matrix perhaps is the main reason why control film (B Film) and the films containing the starch nanoparticles (F and S films) showed similar trend when the temperature increased from 110 °C to 150 °C although the variation of strain with temperature in these films was quite different up to 75 °C.

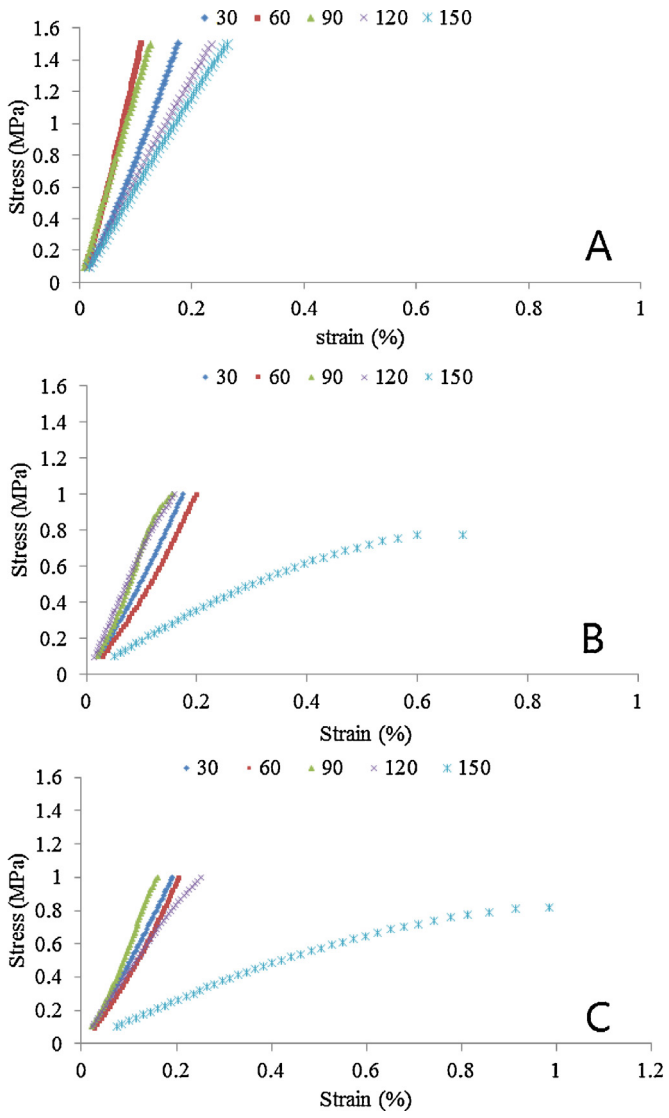

Fig. 5. Stress–strain response of starch films at different temperatures. (A) represents the control (B Film); (B) represents the S Film; (C) represents the F Film.

3.2.2. Young's modulus and toughness of the films

Fig. 5 presents the stress sweep of films containing spray and vacuum freeze dried starch nanoparticles at 30 °C, 60 °C, 90 °C, 120 °C, and 150 °C. The stress sweep of the control film (B Film) at these temperatures is also presented for comparison. Young's modulus (E) and the toughness of these films at different temperature are listed in Tables 2 and 3, respectively. As shown in Fig. 5(A), the stress–strain curves are all linear at these set temperatures and the stress at fracture point is 1.5 MPa. This figure shows that at a given stress, the strain is affected by the temperature. For example, when the stress is 1.4 MPa, the strain of the control film is 0.16% at 30 °C, 0.10% at 60 °C, 0.11% at 90 °C, 0.22% at 120 °C, and 0.24% at 150 °C. These data suggest that the strain decreases with temperature until the film starts to densify due to loss of water from the film matrix. The shrinkage of film, as described in Section 3.2.1, is another reason affecting the strain response (at varying stress) when the temperature remained below 100 °C. However, when the temperature is higher than 100 °C, the softening of starch molecules seemingly enhances the strain response. As shown in Fig. 5(B) and (C), the stress–strain curves of the films containing starch nanoparticles (at all set temperatures) show similar linear trend to in Fig. 5(A) except for the fact that the stress values at which these films fracture are lower than that of the control film. Furthermore, the variation of strain of films containing starch nanoparticles as a function of temperature at (individual) set stress values is also different compared to that of the control film. In the case of the film containing spray dried starch nanoparticles, when the stress was set at 0.9 MPa, the strain values were 0.16%, 0.18%, 0.13% and 0.14% at 30 °C, 60 °C, 90 °C, 120 °C, respectively. This film fractured at 150 °C and the stress and strain values at fracture were 0.77 MPa and 0.68%, respectively. In the case of film containing vacuum freeze dried starch nanoparticles, at a set stress value of 0.9 MPa, the strain values were 0.17%, 0.19%, 0.14%, 0.22% at 30 °C, 60 °C, 90 °C, 120 °C, respectively. This film fractured at 150 °C at stress and strain values of 0.82 MPa and 0.99%, respectively. The presence of starch nanoparticles seemingly facilitates the densification of films containing both starch nanoparticles which could make them brittle. This is the reason why the fracture in nanoparticles containing films occurred at lower stress values than that in the control film.

The Young's modulus values of these films at different temperature are provided in Table 2. As can be seen from this table, the Young's modulus value of films containing spray dried and vacuum freeze dried starch nanoparticles are significantly ($P < 0.05$) lower than that of control film. And the films containing different starch nanoparticles (S and F films) had almost similar Young's modulus ($P > 0.05$). As a typical reflection of ductility, the value of Young's modulus is higher when lager deformation occurs at an applied stress. That means the films containing both the spray dried and vacuum freeze dried nanoparticles are more ductile than the starch-only film.

Table 3 presents the toughness values of the films at different temperature. In the case of starch-only film, the value of toughness decreases from 0.1207 J/m^3 to 0.0762 J/m^3 when the temperature increases from 30 °C to 60 °C and then increases to 0.2013 J/m^3 at 150 °C. For S Film, the toughness value does not vary significantly between 30 °C to 60 °C; however, it decreases significantly ($P < 0.05$) at 90 °C. Finally, the toughness of S Film increased to 0.3403 J/m^3 at 150 °C. The variation of toughness in film containing vacuum freeze dried particles with temperature is also similar, *i.e.*, it does not show significant ($P > 0.05$) difference from 30 °C to 60 °C, then decreases to the lowest value (0.0744 J/m^3) at 90 °C and finally increases to the highest value (0.5017 J/m^3) at 150 °C. At 30 °C, toughness of the control film (0.1207 J/m^3) is significantly ($P < 0.05$) higher compared to the toughness values of films containing spray dried (0.0811 J/m^3) and freeze dried nanoparticles (0.0904 J/m^3). Interestingly, the toughness of this starch only film is significantly ($P < 0.05$) lower than toughness values of the films containing nanoparticles at 60 °C. The results at 90 °C also shows that the toughness of the starch-only film is much higher than those films containing starch nanoparticles as in the case at 30 °C. In contrast the toughness values of the films containing starch nanoparticles at 120 °C and 150 °C were much higher than that of starch only films. At these two temperatures, the toughness values of film containing freeze dried nanoparticles was the highest, that of starch-only film was the lowest and that film containing spray dried nanoparticles remained in between. Toughness is a measure of energy a sample can absorb before it breaks (Parzuchowski, Jurczyk-Kowalska, Ryszkowska, & Rokicki, 2006). The structure and composition of these films are expected to differ with the increase in temperature due to the moisture loss. The differences in the structure and composition are expected to affect the toughness of film. Furthermore, the differences in amorphousness and/or crystallinity in these films are also expected to affect the toughness. From the data presented in Table 3, it can be seen that the presence of starch nanoparticles altered the toughness of these films by altering the internal structure.

Table 2
Young's modulus of starch film with and without starch nanoparticles at different temperatures.[+]

Film type	Young's modulus (GPa)				
	30 °C	60 °C	90 °C	120 °C	150 °C
B Film (control)	8.065 ± 0.678[a]	12.894 ± 0.108[a]	11.924 ± 0.015[a]	6.440 ± 0.007[a]	5.797 ± 0.010[a]
S Film	5.428 ± 0.034[b]	4.707 ± 0.043[b]	6.700 ± 0.060[b]	6.655 ± 0.034[a]	1.475 ± 0.031[b]
F Film	5.025 ± 0.023[b]	4.572 ± 0.039[b]	6.006 ± 0.054[b]	4.198 ± 0.020[b]	1.037 ± 0.021[b]

[+] Values represent the mean ± standard deviation of triplicate tests. Values in columns having different superscripts were significantly different ($P < 0.05$).

Table 3
The toughness of starch films with and without starch nanoparticles at different temperatures.[+]

Film type	Toughness (J/m^3)				
	30 °C	60 °C	90 °C	120 °C	150 °C
B Film (control)	0.1207 ± 0.0028[a]	0.0762 ± 0.0017[a]	0.0939 ± 0.0002[a]	0.1774 ± 0.0001[a]	0.2013 ± 0.0002[a]
S Film	0.0811 ± 0.0009[b]	0.0895 ± 0.0017[b]	0.0784 ± 0.0007[b]	0.0845 ± 0.0005[b]	0.3403 ± 0.0016[b]
F Film	0.0904 ± 0.0010[b]	0.0924 ± 0.0021[b]	0.0744 ± 0.0015[b]	0.1323 ± 0.0008[c]	0.5017 ± 0.0014[c]

[+] Values represent the mean ± standard deviation of triplicate tests. Values in columns having different superscripts were significantly different ($P < 0.05$).

4. Conclusions

Starch films containing spray dried and vacuum freeze dried starch nanoparticles were successfully produced. The physical properties such as morphology, amorphous/crystalline nature, WVP, opacity, T_g and the mechanical properties (strain as a function of stress, Young's modulus, toughness and strain as a function of temperature) were measured. The starch films containing starch nanoparticles had rougher surface, lower WVP and lower T_g and were in amorphous physical state. The starch-only films in the absence of starch nanoparticles had smoother surface, higher crystallinity, higher WVP and higher T_g values. The drying methods used to produce the starch nanoparticles only affected the opacity of the nanoparticles containing starch films. The films containing vacuum freeze dried starch nanoparticles had the highest opacity. The variation of strain with temperature in the films containing both starch nanoparticles was similar. The strain values increased slightly in the start, decreased in 75–110 °C range, and continuously increased in 110–150 °C in all the cases. In the case of starch-only film, there was instantaneous increase in strain in the early stage of temperature sweep experiments followed by very rapid decrease in strain values. The stress values at which the fracture occurred were lower in films containing starch nanoparticles. Both the Young's modulus and toughness of the films were significantly affected by the addition of starch nanoparticles. This manuscript lays foundation in developing biodegradable starch-based films containing starch nanoparticles.

Acknowledgements

This research was supported by National Natural Science Foundation of China (31000813), Chinese Universities Scientific Fund (2012QJ009), High Technology Research and Development Program of China (2011AA100802), Commonweal Guild Agricultural Scientific Research Program of China (201003077), and Science and Technology Program of Beijing (D12110003112002).

References

ASTM. (1987). Standard methods for water vapor transmission of materials (E 96-80). In *Annual book of ASTM standards*. Philadelphia, PA: American Society for Testing and Materials.

Bengtsson, M., Koch, K., & Gatenholm, P. (2003). Surface octanoylation of high-amylose potato starch films. *Carbohydrate Polymers*, *54*, 1–11.

Bourtoom, T., & Chinnan, M. S. (2008). Preparation and properties of rice starch-chitosan blend biodegradable film. *LWT-Food Science and Technology*, *41*, 1633–1641.

Briassoulis, D. (2004). An overview on the mechanical behaviour of biodegradable agricultural films. *Journal of Polymers and the Environment*, *12*(2), 65–81.

Byun, H. S., Park, H. M., Lim, G. T., & Yoon, S. D. (2011). Physical properties and characterization of biodegradable films using nano-sized TiO_2/poly(acrylamide-co-methyl methacrylate) composite. *Journal of Nanoscience and Nanotechnology*, *11*(2), 1701–1705.

Chen, Y., Liu, C.-h., Chang, P. R., Anderson, D. P., & Huneault, M. A. (2008). Pea starch-based composite films with pea hull fibers and pea hull fiber-derived nanowhiskers. *Polymer Engineering & Science*, *49*(2), 369–378.

Cheng, K.-C., Catchmark, J. M., & Demirc, A. (2011). Effects of CMC addition on bacterial cellulose production in a biofilm reactor and its paper sheets analysis. *Biomacromolecules*, *12*, 730–736.

Dai, H.-g., Chang, P. R., Geng, F.-y., Yu, J.-g., & Ma, X.-f. (2010). Preparation and properties of starch-based film using *N*,*N*-bis(2-hydroxyethyl)formamide as a new plasticizer. *Carbohydrate Polymers*, *79*, 306–311.

Follain, N., Joly, C., Dole, P., & Bliard, C. (2005). Properties of starch based blends. Part 2. Influence of poly vinyl alcohol addition and photocrosslinking on starch based materials mechanical properties. *Carbohydrate Polymers*, *60*, 185–192.

Fu, Z.-q., Wang, L.-j., Li, D., Wei, Q., & Adhikari, B. (2011). Effects of high-pressure homogenization on the properties of starch-plasticizer dispersions and their films. *Carbohydrate Polymers*, *86*(1), 202–207.

Galdeano, M. C., Mali, S., Grossmann, M. V. E., Yamashita, F., & García, M. A. (2009). Effects of plasticizers on the properties of oat starch films. *Materials Science and Engineering C*, *29*(2), 532–538.

Glenn, G. M., Imam, S. H., & Orts, W. J. (2011). Starch-based foam composite materials: Processing and bioproducts. *MRS Bulletin*, *36*, 696–702.

Godbole, S., Gote, S., Latkar, M., & Chakrabarti, T. (2003). Preparation and characterization of biodegradable poly-3-hydroxybutyrate-starch blend films. *Bioresource Technology*, *86*, 33–37.

Hu, Y., Topolkaraev, V., Hiltner, A., & Baer, E. (2001). Measurement of water vapor transmission rate in highly permeable films. *Journal of applied polymer science*, *81*(7), 1624–1633.

Jagannath, J. H., Nanjappa, C., Das Gupta, D. K., & Bawa, A. S. (2003). Mechanical and barrier properties of edible starch-protein-based films. *Journal of Applied Polymer Science*, *88*, 64–71.

Jayasekara, R., Harding, I., Bowater, I., Christie, G. B. Y., & Lonergan, G. T. (2004). Preparation, surface modification and characterisation of solution cast starch PVA blended films. *Polymer Testing*, *23*(1), 17–27.

Kampeerapappun, P., Aht-ong, D., Pentrakoon, D., & Srikulkit, K. (2007). Preparation of cassava starch/montmorillonite composite film. *Carbohydrate Polymers*, *67*, 155–163.

Lawal, O. S., Adebowale, K. O., Ogunsanwo, B. M., Barba, L. L., & Ilo, N. S. (2005). Oxidized and acid thinned starch derivatives of hybrid maize: Functional characteristics, wide-angle X-ray diffractometry and thermal properties. *International Journal of Biological Macromolecules*, *35*, 71–79.

Le Corre, D., Bras, J., & Dufresne, A. (2010). Starch nanoparticles: A review. *Biomacromolecules*, *11*, 1139–1153.

Mali, S., Grossmann, M. V. E., García, M. A., Martino, M. N., & Zaritzky, N. E. (2004). Barrier, mechanical and optical properties of plasticized yam starch films. *Carbohydrate Polymers*, *56*, 129–135.

Muscat, D., Adhikari, B., Adhikari, R., & Chaudhary, D. S. (2012). Comparative study of film forming behaviour of low and high amylose starches using glycerol and xylitol as plasticizers. *Journal of Food Engineering*, *109*(2), 189–201.

Pandini, S., Passera, S., Messori, M., Paderni, K., Toselli, M., Gianoncelli, A., et al. (2012). Two-way reversible shape memory behaviour of crosslinked poly(ε-caprolactone). *Polymer*, *53*, 1915–1924.

Parzuchowski, P. G., Jurczyk-Kowalska, M., Ryszkowska, J., & Rokicki, G. (2006). Epoxy resin modified with soybean oil containing cyclic carbonate groups. *Journal of Applied Polymer Science*, *102*, 2904–2914.

Roylance, D. (2001). *Stress–strain curves*. Cambridge, MA: MIT Press.
Ryu, S. Y., Rhim, J. W., Roh, H. J., & Kim, S. S. (2002). Preparation and physical properties of zein-coated high-amylose corn starch film. *Lebensmittel-Wissenschaft und-Technologie*, *35*, 680–686.
Safranski, D. L., Crabtree, J. C., Huq, Y. R., & Gall, K. (2011). Thermo-mechanical properties of semi-degradable poly(b-amino ester)-co-methyl methacrylate networks under simulated physiological conditions. *Polymer*, *52*, 4920–4927.
Saiah, R., Sreekumar, P. A., Leblanc, N., Castandet, M., & Saiter, J. M. (2007). Study of wheat-flour-based agropolymers: Influence of plasticizers on structure and aging behavior. *Cereal Chemistry*, *84*(3), 276–281.
Shi, A.-M., Li, D., Wang, L.-J., Li, B.-Z., & Adhikari, B. (2011). Preparation of starch-based nanoparticles through high-pressure homogenization and miniemulsion cross-linking: Influence of various process parameters on particle size and stability. *Carbohydrate Polymers*, *83*(4), 1604–1610.
Shi, A.-M., Li, D., Wang, L.-J., Zhou, Y.-G., & Adhikari, B. (2012). Spray drying of starch submicron particles prepared by high pressure homogenization and mini-emulsion cross-linking. *Journal of Food Engineering*, *113*(3), 399–407.
Shi, A.-m., Wang, L.-j., Li, D., & Adhikari, B. (2012). The effect of annealing and cryoprotectants on the properties of vacuum-freeze dried starch nanoparticles. *Carbohydrate Polymers*, *88*(4), 1334–1341.
Steward, P. A., Hearn, J., & Wilkinson, M. C. (2000). An overview of polymer latex film formation and properties. *Advances in Colloid and Interface Science*, *86*, 195–267.
Talja, R. A. (2007). *Preparation and characterization of potato starch films plasticized with polyols*. PhD thesis, Department of Food Technology, University of Helsinki.
Vieira, M. G. A., da Silva, M. A., dos Santos, L. O., & Beppu, M. M. (2011). Natural-based plasticizers and biopolymer films: A review. *European Polymer Journal*, *47*, 254–263.
Wilhelm, H.-M., Sierakowski, M.-R., Souza, G. P., & Wypych, F. (2003). Starch films reinforced with mineral clay. *Carbohydrate Polymers*, *52*, 101–110.
Wittaya, T. (2009). Microcomposites of rice starch film reinforced with microcrystalline cellulose from palm pressed fiber. *International Food Research Journal*, *16*, 493–500.
Xiong, H.-g., Tang, S.-w., Tang, H.-l., & Zou, P. (2008). The structure and properties of a starch-based biodegradable film. *Carbohydrate Polymers*, *71*, 263–268.
Yun, T.-H., & Yoon, S.-D. (2010). Effect of amylose contents of starches on physical properties and biodegradability of starch/PVA-blended films. *Polymer Bulletin*, *64*, 553–568.
Zhai, M.-l., Zhao, L., Yoshii, F., & Kume, T. (2004). Study on antibacterial starch/chitosan blend film formed under the action of irradiation. *Carbohydrate Polymers*, *57*, 83–88.